

Blurring the Lines Between Host and Guest: A Chimeric Receptor Derived from Cucurbituril and Triptycene

Xiaoyong Lu, Soumen K. Samanta, Peter Y. Zavalij, and Lyle Isaacs*

Dedication ((optional))

Abstract: We report the synthesis and x-ray crystal structure of cucurbituril–tritycene chimeric receptor (**1**). Host **1** binds to guests typical of CB[6] – CB[8], but also binds to larger guests like blue box (**20**) and the Fujita square (**22**). Intriguingly, the geometries of the **1**•**20** and **1**•**22** complexes blur the lines between host and guest in that both components fulfill both roles within each complex. The fluorescence output of **1** is fully quenched by the formation of complexes with pyridinium derived guests **12** and **19**.

The construction of complex and functional architectures both in science and in everyday life requires the availability of a diverse array of building blocks. Within the realm of supramolecular chemistry these building blocks – often planar (hetero)aromatic rings – are connected to form macrocyclic oligomeric hosts by covalent bonds or non-covalent interactions and serve as receptors for chemically and biologically important guests.^[1] Advanced systems incorporate these hosts into more complex architectures (e.g. rotaxanes) to create optical sensors, drug delivery vehicles, molecular electronics and molecular machines.^[2] Among the most widely used host systems are the cyclodextrins, calixarenes, crown ethers, cyclophanes, pillararenes, coordination cages, and capsules.^[3] In recent years, cucurbit[n]uril (CB[n]) hosts – derived from the non-planar, non-aromatic building block glycoluril – have been embraced by the supramolecular chemistry community as a next generation host system because they form high affinity, highly selective, and stimuli responsive host•guest complexes (Figure 1).^[2a, 4] We have recently created acyclic but preorganized CB[n]-type receptors (e.g. **M1**) and studied their function as solubilizing agents for insoluble drugs and as *in vivo* reversal agents for neuromuscular blocking drugs.^[5] The groups of Klärner, Schrader, and Yoshizawa have prepared beautiful water soluble C-shaped receptors based on norbornene and anthracene buildings, respectively.^[6] We drew inspiration from the work of Chen, Swager, and others on the use of triptycene as a building block for molecular and polymeric materials for molecular recognition and (fluorescence) sensing applications.^[7] In this paper, we report the preparation of chimeric receptor (**1**) that combines that desirable recognition properties of CB[n]-type and triptycene derived receptors.

The preparation of triptycene host **1** follows our building block approach (Figure 1).^[5a, 8] To prepare a triptycene based aromatic wall we performed the Diels-Alder reaction between

anthracene (**2**) and benzoquinone (**3**) followed by aromatization under acidic conditions to yield **4** in 66% yield over both steps.^[9] Next, we allowed **4** to react with 1,3-propanesultone (**5**) under basic conditions (NaOH, dioxane / H₂O) to give aromatic wall **6** in 75% yield. Finally, the double electrophilic aromatic substitution reaction between aromatic wall **6** and glycoluril tetramer **7** was performed (TFA, Ac₂O (1:1)) which gave triptycene host **1** in 30% yield after purification by silica gel chromatography and gel permeation chromatography (Sephadex G25). Host **1** was characterized by electrospray ionization mass spectrometry as well as ¹H and ¹³C NMR spectroscopy which provide strong evidence for the molecular formula and time averaged C_{2v}-symmetry of **1** (Supporting Information). The solubility of host **1** in water (≈ 3 mM) is sufficient to allow an investigation of its molecular recognition properties (*vide infra*).

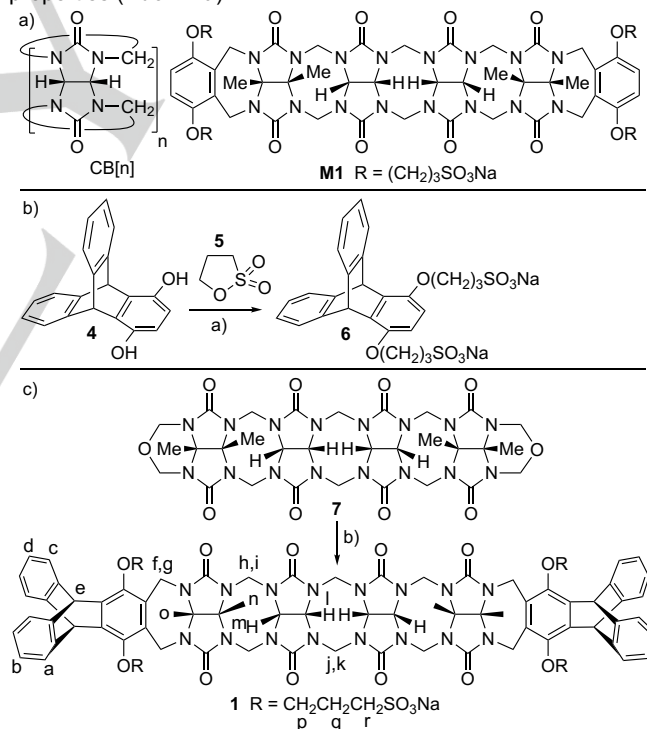


Figure 1. a) Chemical structures of CB[n] and **M1**. Synthesis of: b) triptycene wall **6** and c) triptycene host **1**. Conditions: a) NaOH, dioxane/H₂O, RT, 15 h, 75%, b) TFA / Ac₂O (1:1), 95 °C, 4 h, 30%.

We were fortunate to obtain x-ray crystal structures of both aromatic wall **6** (CCDC 1829725) and triptycene host **1** (CCDC 1829724) as shown in Figure 2.^[10] Figure 2a shows the packing of **6** in the crystal along the a-axis. Interestingly, two molecules of **6** associate with one another by π-π interactions (mean interplanar separation of 3.57 Å) between the dialkoxy substituted aromatic walls. In addition, one of the unsubstituted

[*] Dr. Xiaoyong Lu, Dr. Soumen K. Samanta, Dr. Peter Y. Zavalij, Prof. Dr. Lyle Isaacs
Department of Chemistry and Biochemistry
University of Maryland
College Park, MD 20742 (USA)
E-mail: LIsaacs@umd.edu
Supporting information and the ORCID identification number(s) for the author(s) of this article can be found under <http://dx.doi.org/xxxxxxx>

aromatic blades of triptycene **6** nestles into the cleft of an adjacent molecule in a geometry reminiscent of the stack of shuttlecocks. Quite interestingly, triptycene host **1** assumes a lower symmetry conformation whereby one unsubstituted aromatic ring folds into its cavity and reduces the overall cavity volume (Figure 2b). These two aromatic rings are not coplanar and the Ar C-atom to mean plane distances range from 3.55 – 3.86 Å (Figure 2b) which is longer than the optimal π - π stacking distance of \approx 3.4 Å. The cavity of **1** is filled with $\text{CF}_3\text{CO}_2\text{H}$. The packing of **1** in the crystal is even more interesting. Three molecules of **1** form a trimer in the ab-plane that again features

a shuttlecock type arrangement between the tips of the unsubstituted aromatic rings of the triptycene walls (Figure 2c). Finally, these trimers are linked together by Na^+ ions that bridge between the ureidyl C=O groups to form a hexagonal honeycomb-type network (Figure 2d). The solvent filled holes in the hexagonal honeycomb-type network form continuous solvent filled channels that extend along the c-axis in the crystal. Overall, the packing of **1** in the crystal can be seen as a direct consequence of the preferences of its acyclic CB[n] and triptycene components.

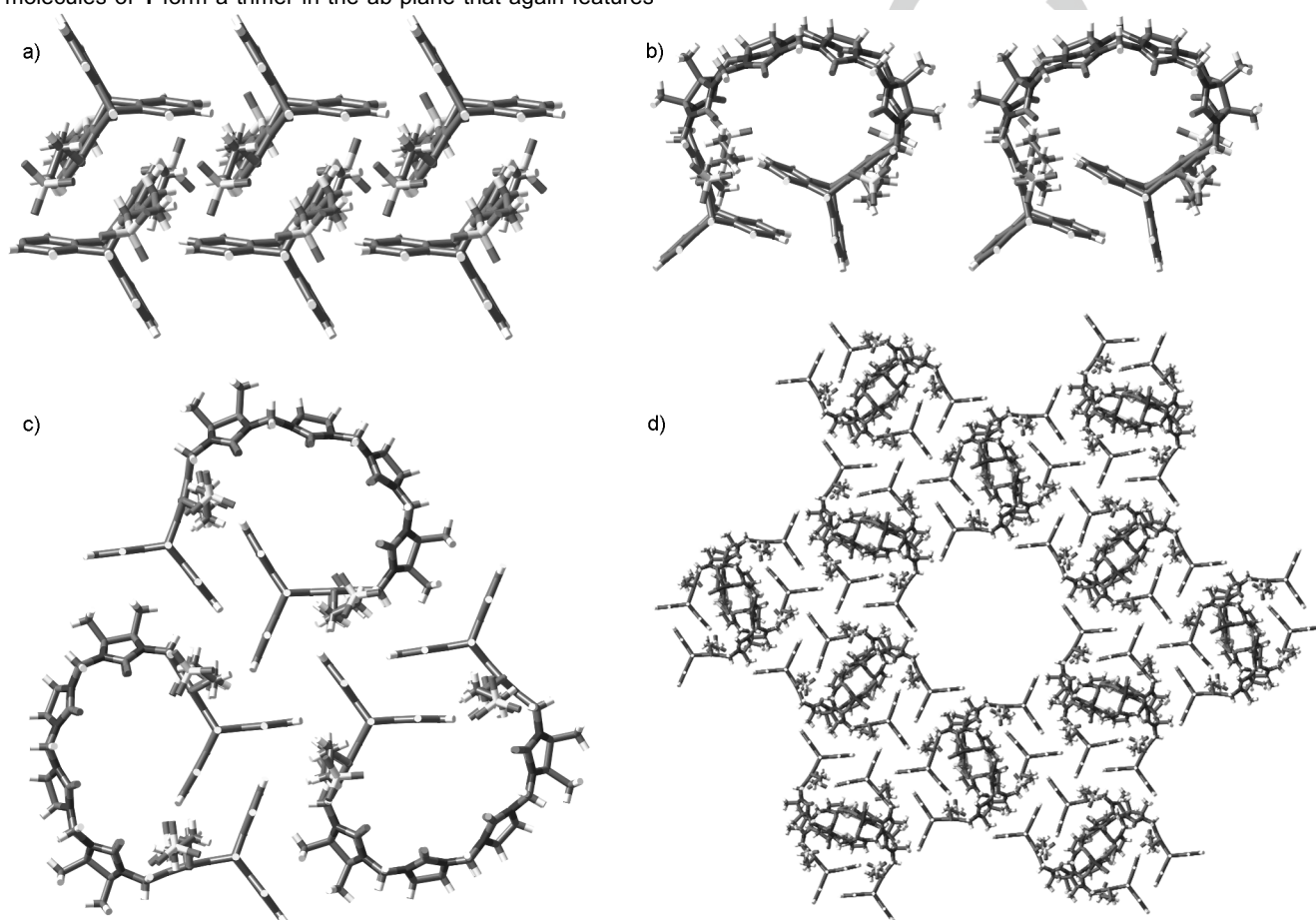


Figure 2. Representations of the x-ray crystal structures of: a) aromatic wall **6**. b) Stereoview of an individual molecule of **1** in the crystal. c) Packing of three molecules of **1** to give a trimer packing motif. d) Packing of six trimer motifs resulting in a hexagonal channel packing motif.

Given the propensity of **1** for self-assembly in the crystal we first sought to determine if **1** is also trimeric in solution.^[11] Accordingly, we performed a ^1H NMR dilution experiment (3 mM to 0.03 mM, Supporting Information Figure S40) but did not observe any significant changes in chemical shift. In addition, we measured the diffusion coefficients for **1** alone ($D = 2.45 \times 10^{-10} \text{ m}^2 \text{ s}^{-1}$) and for monomeric **1**•**12** complex ($D = 2.57 \times 10^{-10} \text{ m}^2 \text{ s}^{-1}$). Having established that **1** remains monomeric in water below its solubility limit of \approx 3 mM, we next turned our attention to exploring the recognition properties of triptycene host **1**. Based on the structure of **1** whose cavity is shaped by four glycoluril rings and four aromatic rings we envisioned that **1**

might be able to accommodate voluminous guests. Conversely, the x-ray crystal structure of **1** (Figure 2b) shows a smaller cavity with a self-folded conformation based on π - π interactions that would need to be interrupted to accommodate larger guests. Accordingly, we decided to investigate the interaction of **1** with guests **8** – **19** (Figure 3) which differ greatly in size. We started with narrow guest **13** with a hexylene linker which is appropriate for a CB[6] sized cavity. Figure 4a-c shows the ^1H NMR spectra recorded for **1** alone and for 1:1 and 1:2 mixtures of **1** and **13**. In Figure 4a, the resonances for H_c and H_d of the triptycene wall are upfield of those for H_a and H_b which likely reflects the shielding effect of the opposing triptycene wall in the π -stacked

geometry shown in Figure 2b. Interestingly, when the ^1H NMR spectrum of **1** was recorded in DMSO- d_6 , H_c and H_d resonate at 7.44 and 7.12 ppm, respectively, which suggests that the π -stacking between triptycene walls is disrupted in this solvent. The large upfield shifts observed for H_u and H_v (Figure 4b; \square ; H_s : -0.25, H_t : -0.17, H_u : -1.25, H_v : -2.03 ppm) within the **1**·**13** complex reflect the anisotropic shielding effect of the four aromatic rings that help define the cavity of **1** whereas the observation of separate resonances for both free and bound **13** (Figure 4c) establishes the slow nature of guest exchange on the chemical shift time scale. Interestingly, the host resonances $\text{H}_a - \text{H}_d$, H_n , and H_o undergo downfield shifts upon complexation which may reflect the disruption of the self-folded geometry (Figure 4a).

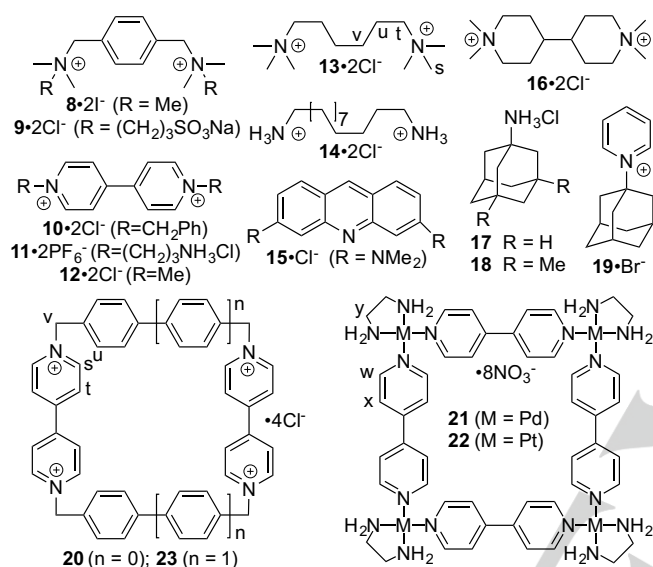


Figure 3. Chemical structures of guests **8** – **23** used in this study.

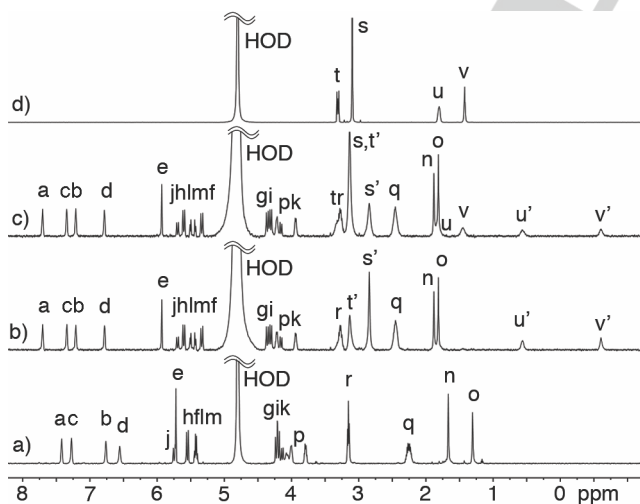


Figure 4. ^1H NMR spectra (600 MHz, D_2O , 298K) recorded for solution of: a) host **1** (0.2 mM), b) mixture of host **1** (0.2 mM) and guest **13** (0.2 mM); c) mixture of host **1** (0.2 mM) and guest **13** (0.4 mM); d) guest **13** (0.4 mM).

Next, we investigated wider guests **8** and **9** with a *p*-phenylene linker which are appropriate for CB[6] and CB[7] sized cavities. ^1H NMR experiments show slow exchange kinetics of binding and large upfield shifts for the Ar-H of guests **8** and **9** (\square = -1.52

and -1.53 ppm) when complexed to **1** (Supporting Information) which establishes binding inside the cavity of **1**. Even larger guests, which are typical of CB[7] or CB[8] sized cavities (viologens **10** – **12**, dye **15**, 4,4'-dipiperidinium **16**, adamantane derivatives **17** and **19**) also bind inside the cavity of **1** and show significant upfield shifts of the guest protons upon binding (Supporting Information) although the larger adamantane derived guests **17** – **19** display fast exchange kinetics on the chemical shift timescale. To gain quantitative information on the strength of host-guest binding we performed isothermal titration microcalorimetry experiments between **1** and guests **10**, **12**, **13**, and **17** (Supporting Information and Table 1) which show enthalpically dominated binding events with K_a values in the 10^6 – 10^7 M^{-1} range. The dominant enthalpic driving force observed complexes of **1** likely reflects the presence of high energy waters similar to the situation recently delineated for macrocyclic CB[n] receptors.^[12] Interestingly, adamantane ammonium guest **17** which is an ultratight guest for CB[7] binds more than 20-fold weaker to **1** than aromatic guests **10**, **12**, and **13** which likely reflects the competing recognition preferences of the chimeric host **1** (e.g. CB[n]-type regions prefer alicyclic guests *versus* triptycene regions which prefer aromatics).

Table 1. Binding constants and thermodynamic parameters for host **1** and selected guests.

Guest	K_a (M^{-1})	ΔG (kcal mol^{-1})	ΔH (kcal mol^{-1})	$-\Delta S$ (kcal mol^{-1})
10 ^a	$3.5 \pm 0.4 \times 10^7$	-10.3	-10.1 ± 0.08	-0.19
12 ^a	$2.8 \pm 0.4 \times 10^7$	-9.0	-18.1 ± 0.3	9.09
13 ^a	$2.6 \pm 0.4 \times 10^7$	-10.1	-8.89 ± 0.08	-1.23
17 ^a	$1.4 \pm 0.1 \times 10^6$	-8.4	-4.86 ± 0.4	-3.54
20 ^a	$3.7 \pm 0.2 \times 10^7$	-10.5	-10.1 ± 0.1	-0.46
22 ^b	$1.2 \pm 0.2 \times 10^6$	-8.3	-11.3 ± 0.14	3.05

Note. ^[a] H_2O , 25 °C. ^[b] 20 mM sodium phosphate buffered H_2O containing 1M NaNO_3 , pH 7.4, 25 °C.

Subsequently, we sought to test the limits of the capacity of host **1** by offering it guests that are too large to fit inside macrocyclic CB[8] which is also composed of eight building blocks. An obvious choice was blue box **20** which is known to bind CB[10] but not CB[8].^[13] Accordingly, we titrated an aqueous solution of **1** with **20** and observed the formation of a precipitate that contained a 1:1 mixture of the components. We believe the poor solubility of the **1**·**20** complex reflects the formation of a zwitterion (e.g. tetraanion **1** complexed with tetracation **20**). Although the poor solubility of **1**·**20** in water prevented use of ^1H NMR as an analytical tool, we were able to measure the K_a value for **1**·**20** by ITC ($3.7 \pm 0.2 \times 10^7$ M^{-1}) by using low concentrations of **1** (8.75 μM) in the ITC cell. Fortunately, we found that the **1**·**20** complex is stable in 30% DMSO- d_6 in D_2O which allowed us to record the ^1H NMR spectra shown in Figure 5 which could be assigned with the help of the COSY and NOESY spectra (Supporting Information). Most interesting is that the symmetry of both the host and the guest are reduced (and the number of resonances increased) upon formation of the **1**·**20** complex. For example, host **1** exhibits four resonances for CH_3 -groups n and o, five pairs of resonances for the diastereotopic CH_2 -groups of the glycoluril tetramer

backbone, four resonances for H_l and H_m , and four sets of resonances for the aromatic triptycene walls which indicates that the two ends of host **1** are different in complex **1**•**20**. Similarly, two sets of upfield shifted resonances are observed for each of the viologen protons H_s and H_t of **20** (δ : $s = -0.27$ and -0.38 ppm; $t = -0.73$ and -2.29 ppm) in the **1**•**20** complex. One aromatic wall (Ar4, Figure 5) and one viologen proton (H_s) are strongly upfield shifted by cavity inclusion. These observations are not consistent with a geometry where guest **20** is fully engulfed by host **1** but rather point to a geometry whereby one of the aromatic walls of **1** (Ar4) inserts into the cavity of blue box **20** and one of the viologen units of **20** inserts into the cavity of **1** as depicted in Figure 6a. Cross peaks observed in the 2D NOESY spectrum are consistent with this geometrical assignment (Supporting Information). We find this geometry to be intriguing because it blurs the typical lines of division between host and guest in that regions of **1** and **20** perform both host and guest roles within a single structure. In analogy with the clipped rotaxane previously reported by Klärner,^[14] the geometry of **1**•**20** can be viewed as a clipped catenane.

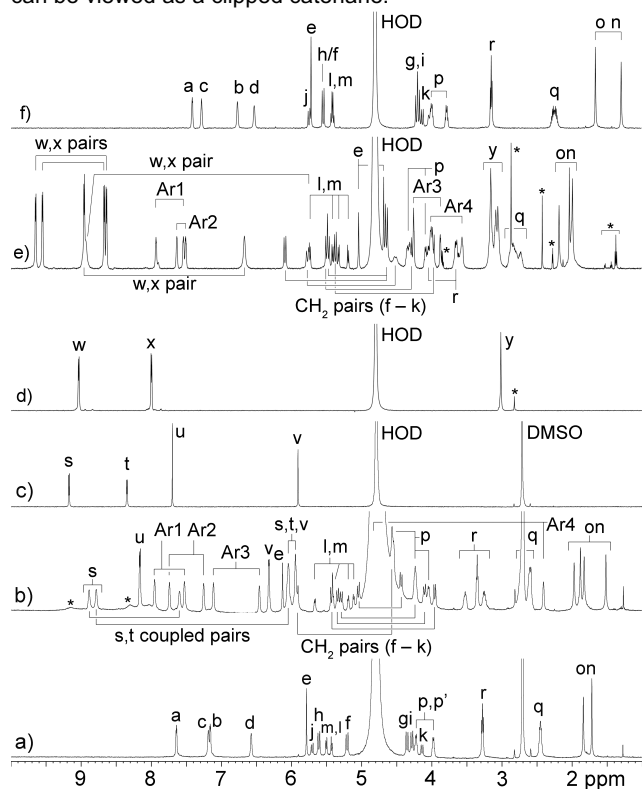


Figure 5. ^1H NMR spectra (600 MHz, 298K) recorded for: a) **1** (0.5 mM), b) a mixture of **1** (0.5 mM) and **20** (0.6 mM), and c) **20** (0.5 mM) in 30% $\text{DMSO}-d_6$ in D_2O , and for d) **22** (0.2 mM), e) a mixture of **22** (0.2 mM) and **1** (0.2 mM), and f) **1** (0.2 mM) in D_2O containing 2 M NaNO_3 . * = trace impurities.

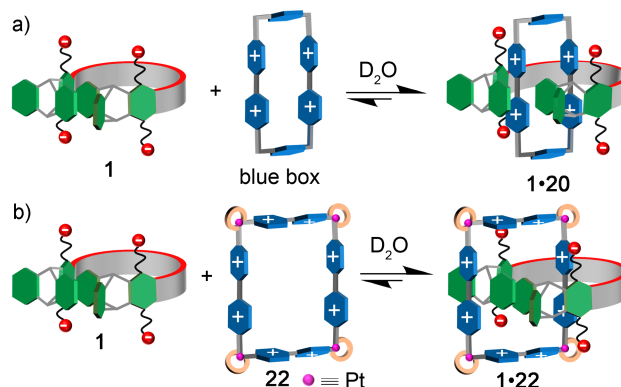


Figure 6. Depictions of the proposed geometries of: a) **1**•**20**, and b) **1**•**22**.

Encouraged by the intriguing geometry of the **1**•**20** complex, we decide to investigate the binding of **1** with Fujita's bipyridine squares (**21**: $M = \text{Pd}$, and **22**: $M = \text{Pt}$).^[15] After much experimentation, on the basis of ^1H NMR titration and ITC experiments (Supporting Information) and considering the kinetic lability of the $\text{Pd}-\text{N}$ coordination bonds^[15] we determined that addition of four equivalents of **1** to a solution of **21** causes its disassembly into four equivalents of bipyridine• $\text{Pd}(\text{en})$ which bind to **1** in the usual way. The situation was completely different for the platinum analogue **22** because of its kinetically inert $\text{Pt}-\text{N}$ coordination bonds.^[15] Figure 5d-f shows the ^1H NMR spectra recorded in D_2O for **1**, **22**, and the **1**•**22** complex. Assignments are based on the variable temperature, COSY and NOESY spectra (Supporting Information). As observed previously with blue box, the symmetry of both **1** and **22** are reduced upon formation of the **1**•**22** complex. For example, the four chemically equivalent bipyridine units of **22** show only two resonances (H_w and H_x) but eight are observed for the **1**•**22** complex suggesting clipping of **1** onto one bipyridine unit of **22**. Similarly, host **1** within the **1**•**22** shows four resonances for CH_3 -groups n and o , four resonances for H_l and H_m , two resonances for H_e , and five pairs of resonances for the CH_2 -groups of the glycoluril tetramer backbone ($H_f - H_k$), again indicating the end-to-end asymmetric nature of **1** within the **1**•**22** complex. In contrast to **1**•**20**, two of the aromatic walls of **1** are substantially upfield shifted upon formation of **1**•**22** which suggests that both are bound within the cavity of **22**. In accord with all of the NMR evidence, we propose that **1**•**22** adopts the geometry depicted in Figure 6b. Once again, the distinction between host and guest is blurry in that two aromatic walls of **1** fill the cavity of **22** whereas one bipyridine wall of **22** binds inside the cavity of **1**. Stoddart's covalent square **23** forms complex **1**•**23** whose structure is analogous to that of **1**•**22**.

Beyond the intriguing geometrical features of the complex between **1** and **20** or **22** lies interesting optical properties. Initially, we found that wall **2** absorbs at 213 nm ($\epsilon = 4.7 \times 10^4 \text{ M}^{-1} \text{ cm}^{-1}$). Compound **2** is fluorescent with an emission band at 337 nm ($\lambda_{\text{ex}} = 213 \text{ nm}$). The fluorescence of **2** is quenched by the addition of Fe^{3+} , partially quenched by Cu^{2+} , but not Ag^+ and NH_4^+ (Supporting Information). In contrast, host **1** displays a UV/Vis absorbance band at 214 nm ($\epsilon = 6.6 \times 10^4 \text{ M}^{-1} \text{ cm}^{-1}$) and a longer wavelength fluorescence emission maximum at 377 nm in water which is probably due to interaction between the two

tritycene walls. Accordingly, we hypothesized that guest binding might lead to significant fluorescence changes. Figure 7 shows the fluorescence spectra recorded for **1** (12 μM) in the presence of different guests and Table 2 presents key parameters. Interestingly, in all cases guest binding results in a hypsochromic shift in emission maximum probably due to disruption in the $\pi\text{-}\pi$ interactions between the tritycene walls. Most interesting is the divergent behavior of adamantane derivatives **17**, **18**, and **19**. Whereas the **1**·**17** and **1**·**18** complexes display enhanced fluorescence, complex **1**·**19** is completely quenched presumably due to photoinduced electron transfer from the excited state of **1** to the pyridinium guest **19**. In accord with this interpretation is the observation that methyl viologen complex **1**·**12** is also heavily quenched. Related sensing materials have been pioneered by Swager for detection of nitroaromatics.^[16] Host **1** and related compounds – with their high affinity and selectivity toward hydrophobic cations – may offer unique opportunities as aqueous sensors for pyridinium and related quaternary ammoniums that are present in drugs and other natural products (e.g. NADP).

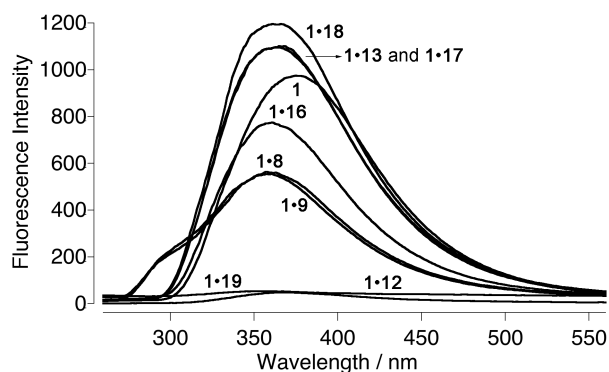


Figure 7. Fluorescence spectra ($\lambda_{\text{ex}} = 214 \text{ nm}$, 298 K, H_2O) recorded for **1** (12 μM) in the presence of 2.0 equivalent of guests (**8**, **9**, **13**, **16**, **17**, **18**, **19**).

Table 2. Guest induced fluorescence change of **1** ($\lambda_{\text{ex}} = 214 \text{ nm}$, 298 K).

Host	1 ·guest						
	8	9	13	16	17	18	19
1							
λ_{em} (nm)	377	357	360	368	361	363	366
$\Delta\lambda_{\text{em}}$ (nm)	0	-20	-17	-9	-16	-14	-11
$(I/I_0)\%$	100	58	57	113	79	112	123
$\Phi(\%)$	6.9	2.6	4.3	7.6	3.5	5.5	8.8

In summary, we have reported the synthesis of a chimeric receptor **1** combining the recognition preferences of the cucurbituril and triptycene. The x-ray crystal structure of **1** reveals a self-folded geometry based on $\pi\text{-}\pi$ interactions between the triptycene walls of **1**; **1** further organizes itself into a honeycomb arrangement that features infinite solvent filled channels along the c-axis. Host **1** binds to hydrophobic (di)cations as is typical of CB[n] derived receptors but also recognized larger guests like blue box **20** and Fujita square **22**. Intriguingly, the geometries of **1**·**20** and **1**·**22** blur the lines

between what constitutes host and guest in that each component contains binding epitopes that fulfil both roles in each complex. Finally, **1** displays guest responsive fluorescence and is particularly sensitive to pyridinium derived guests **12** and **19** which quench host fluorescence by photoinduced electron transfer. Overall, the work further establishes acyclic CB[n]-type receptors as versatile and readily functionalized systems that display both intriguing recognition behaviour and function.

Acknowledgements

We thank the US National Science Foundation (CHE-1404911 and CHE-1807486) for financial support.

Keywords: cucurbituril • host-guest systems • triptycene • supramolecular chemistry • fluorescence

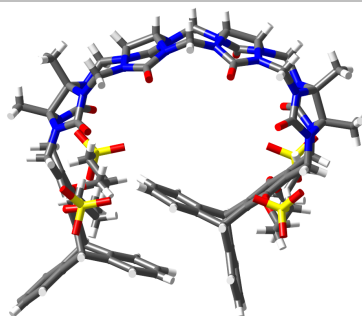
- [1] D. J. Cram, *Angew. Chem., Int. Ed. Engl.* **1988**, *27*, 1009-1020.
 [2] a) G. Ghale, W. M. Nau, *Acc. Chem. Res.* **2014**, *47*, 2150-2159; b) L. You, D. Zha, E. V. Anslyn, *Chem. Rev.* **2015**, *115*, 7840-7892; c) E. J. Dale, N. A. Vermeulen, M. Juricek, J. C. Barnes, R. M. Young, M. R. Wasielewski, J. F. Stoddart, *Acc. Chem. Res.* **2016**, *49*, 262-273; d) E. R. Kay, D. A. Leigh, *Angew. Chem., Int. Ed.* **2015**, *54*, 10080-10088; e) E. Kim, D. Kim, H. Jung, J. Lee, S. Paul, N. Selvapalam, Y. Yang, N. Lim, C. G. Park, K. Kim, *Angew. Chem., Int. Ed.* **2010**, *49*, 4405-4408; f) S. J. Barrow, S. Kaser, M. J. Rowland, J. del Barrio, O. A. Scherman, *Chem. Rev.* **2015**, *115*, 12320-12406; g) G. Yu, K. Jie, F. Huang, *Chem. Rev.* **2015**, *115*, 7240-7303; h) M.-X. Wu, Y.-W. Yang, *Adv. Mater.* **2017**, 1606134; i) A. Coskun, J. M. Spruell, G. Barin, W. R. Dichtel, A. H. Flood, Y. Y. Botros, J. F. Stoddart, *Chem. Soc. Rev.* **2012**, *41*, 4827-4859.
 [3] a) F. Diederich, *Angew. Chem., Intl. Ed. Engl.* **1988**, *27*, 362-386; b) M. Xue, Y. Yang, X. Chi, Z. Zhang, F. Huang, *Acc. Chem. Res.* **2012**, *45*, 1294-1308; c) J. Rebek, *Acc. Chem. Res.* **2009**, *42*, 1660-1668; d) S. Zarra, D. M. Wood, D. A. Roberts, J. R. Nitschke, *Chem. Soc. Rev.* **2015**, *44*, 419-432; e) L. Szentei, J. Szejtli, *Adv. Drug Delivery Rev.* **1999**, *36*, 17-28; f) C. D. Gutsche, *Acc. Chem. Res.* **1983**, *16*, 161-170; g) C. J. Pedersen, *Angew. Chem. Int. Ed. Engl.* **1988**, *27*, 1021-1027.
 [4] a) L. Isaacs, *Acc. Chem. Res.* **2014**, *47*, 2052-2062; b) Y. H. Ko, E. Kim, I. Hwang, K. Kim, *Chem. Commun.* **2007**, 1305-1315; c) J. Del Barrio, P. Horton, D. Lairez, G. Lloyd, C. Toprakcioglu, O. Scherman, *J. Am. Chem. Soc.* **2013**, *135*, 11760-11763.
 [5] a) D. Ma, G. Hettiarachchi, D. Nguyen, B. Zhang, J. B. Wittenberg, P. Y. Zavalij, V. Briken, L. Isaacs, *Nat. Chem.* **2012**, *4*, 503-510; b) D. Ma, B. Zhang, U. Hoffmann, M. G. Sundrup, M. Eikermann, L. Isaacs, *Angew. Chem., Int. Ed.* **2012**, *51*, 11358-11362.
 [6] a) P. Talbiersky, F. Bastkowski, F.-G. Klärner, T. Schrader, *J. Am. Chem. Soc.* **2008**, *130*, 9824-9828; b) D. Bier, R. Rose, K. Bravo-Rodríguez, M. Bartel, J. M. Ramirez-Anguila, S. Dutt, C. Wilch, F.-G. Klärner, E. Sanchez-Garcia, T. Schrader, C. Ottman, *Nat. Chem.* **2013**, *5*, 234-239; c) K. Jono, A. Suzuki, M. Akita, K. Albrecht, K. Yamamoto, M. Yoshizawa, *Angew. Chem. Int. Ed.* **2017**, *56*, 3570-3574.
 [7] a) X. Liu, Z. J. Weinert, M. Sharafi, M. Liao, J. Li, S. T. Schneebeli, *Angew. Chem. Int. Ed.* **2015**, *54*, 12772-12776; b) K. Lou, A. M. Prior, B. Wiredu, J. Desper, D. H. Hua, *J. Am. Chem. Soc.* **2010**, *132*, 17635-17641; c) J. H. Chong, M. J. MacLachlan, *Chem. Soc. Rev.* **2009**, *38*, 3301-3315; d) Y. Han, Z. Meng, Y.-X. Ma, C.-F. Chen, *Acc. Chem. Res.* **2014**, *47*, 2026-2040; e) T. M. Swager, *Acc. Chem. Res.* **2008**, *41*, 1181-1189.
 [8] B. Zhang, L. Isaacs, *J. Med. Chem.* **2014**, *57*, 9554-9563.

- [9] a) J. R. Wiegand, Z. P. Smith, Q. Liu, C. T. Patterson, B. D. Freeman, R. Guo, *J. Mater. Chem. A* **2014**, *2*, 13309-13320; b) Y. Liu, S. R. Turner, G. Wilkes, *Macromolecules* **2011**, *44*, 4049-4056.
- [10] CCDC 1829725 (wall **6**) and CCDC 1829724 (host **1**) contain the supplementary crystallographic data for this paper. These data can be obtained free of charge from The Cambridge Crystallographic Data Centre via http://www.ccdc.cam.ac.uk/data_request/cif.
- [11] L. Ustrnul, M. Babiak, P. Kulhanek, V. Sindelar, *J. Org. Chem.* **2016**, *81*, 6075-6080.
- [12] a) W. M. Nau, M. Florea, K. I. Assaf, *Isr. J. Chem.* **2011**, *51*, 559-577; b) F. Biedermann, V. D. Uzunova, O. A. Scherman, W. M. Nau, A. De Simone, *J. Am. Chem. Soc.* **2012**, *134*, 15318-15323; c) F. Biedermann, W. M. Nau, H.-J. Schneider, *Angew. Chem., Int. Ed.* **2014**, *53*, 11158-11171.
- [13] W. Gong, X. Yang, P. Y. Zavalij, L. Isaacs, Z. Zhao, S. Liu, *Chem. - Eur. J.* **2016**, *22*, 17612-17618.
- [14] F.-G. Klärner, U. Burkert, M. Kamieth, R. Boese, *J. Phys. Org. Chem.* **2000**, *13*, 604-611.
- [15] M. Fujita, F. Ibukuro, K. Yamaguchi, K. Ogura, *J. Am. Chem. Soc.* **1995**, *117*, 4175-4176.
- [16] J.-S. Yang, T. M. Swager, *J. Am. Chem. Soc.* **1998**, *120*, 11864-11873.

Entry for the Table of Contents

COMMUNICATION

Blurring the Lines: We report the preparation, x-ray crystal structure, and molecular recognition properties of cucurbituril–triptycene chimeric receptor **1**.



*Xiaoyong Lu, Soumen K. Samanta,
Peter Y. Zavalij, Lyle Isaacs**

Page No. – Page No.

**Blurring the Lines Between Host and
Guest: A Chimeric Receptor Derived
from Cucurbituril and Triptycene**